Supplemental Information

3D-Printed Flow Distributor with Uniform Flow Rate Control for Multi-Stacking Microfluidic Systems

Young-June Park, Taejong Yu, Se-Jun Yim, Donghyun You*, and Dong-Pyo Kim*

*Corresponding authors:

- Dong-Pyo Kim

Center of Intelligent Microprocess for Pharmaceutical Synthesis, Department of Chemical Engineering, Pohang University of Science and Technology, Environ. Eng. Bldg., San 31, Hyoja-dong, Nam-gu, Pohang, Korea

Tel.: +82-54-279-2272; fax: +82-54-279-5598.

E-mail address: dpkim@postech.ac.kr.

- Donghyun You

Department of Mechanical Engineering, Pohang University of Science and Technology, Mechanical Eng. Bldg., San 31, Hyoja-dong, Nam-gu, Pohang, Korea

Tel.: +82-54-279-2191; fax: +82-54-279-3199.

E-mail address: dhyou@postech.ac.kr.

1. Tube connection of 3D printed microfluidic system

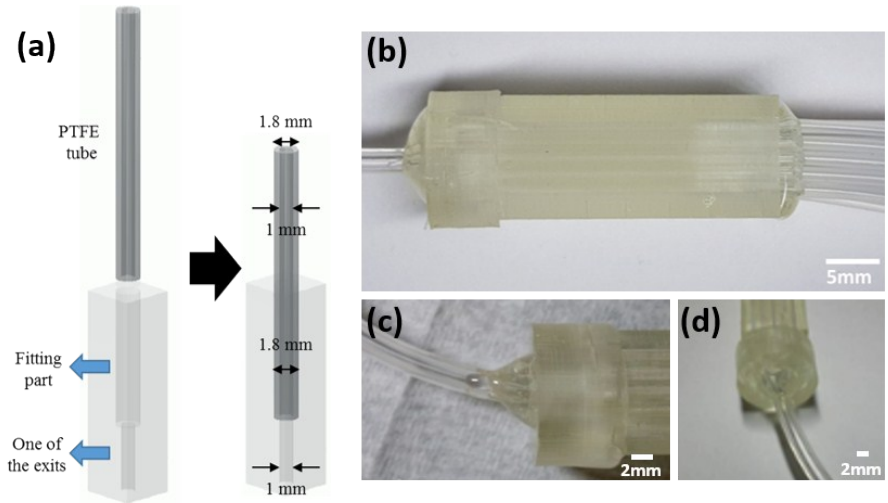

Fig. S1 (a) Scheme of the tube connection for each exit channel with specific dimensions. (b) Images of 3D printed devices with tube connection using epoxy glue bonding at both a single inlet and 25 exit channels, and (c, d) enlarged images of the inlet part.

2. Schematic diagram of experimental system set up

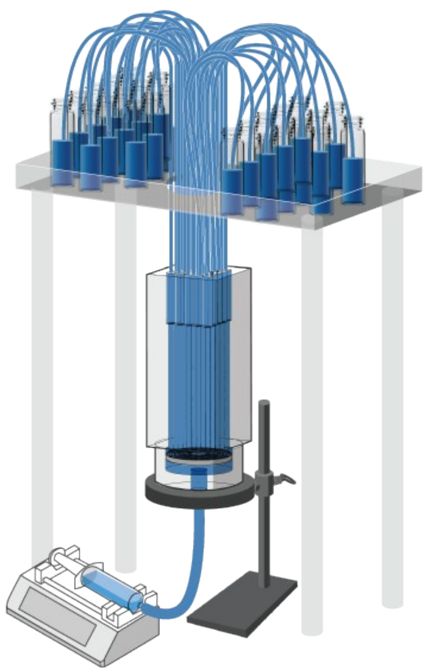

Scheme S1 Scheme of an experiment set for a single inlet distributed into 25 vials through a flow distributor.

3. Computational configurations of optimization procedure and average velocity distribution

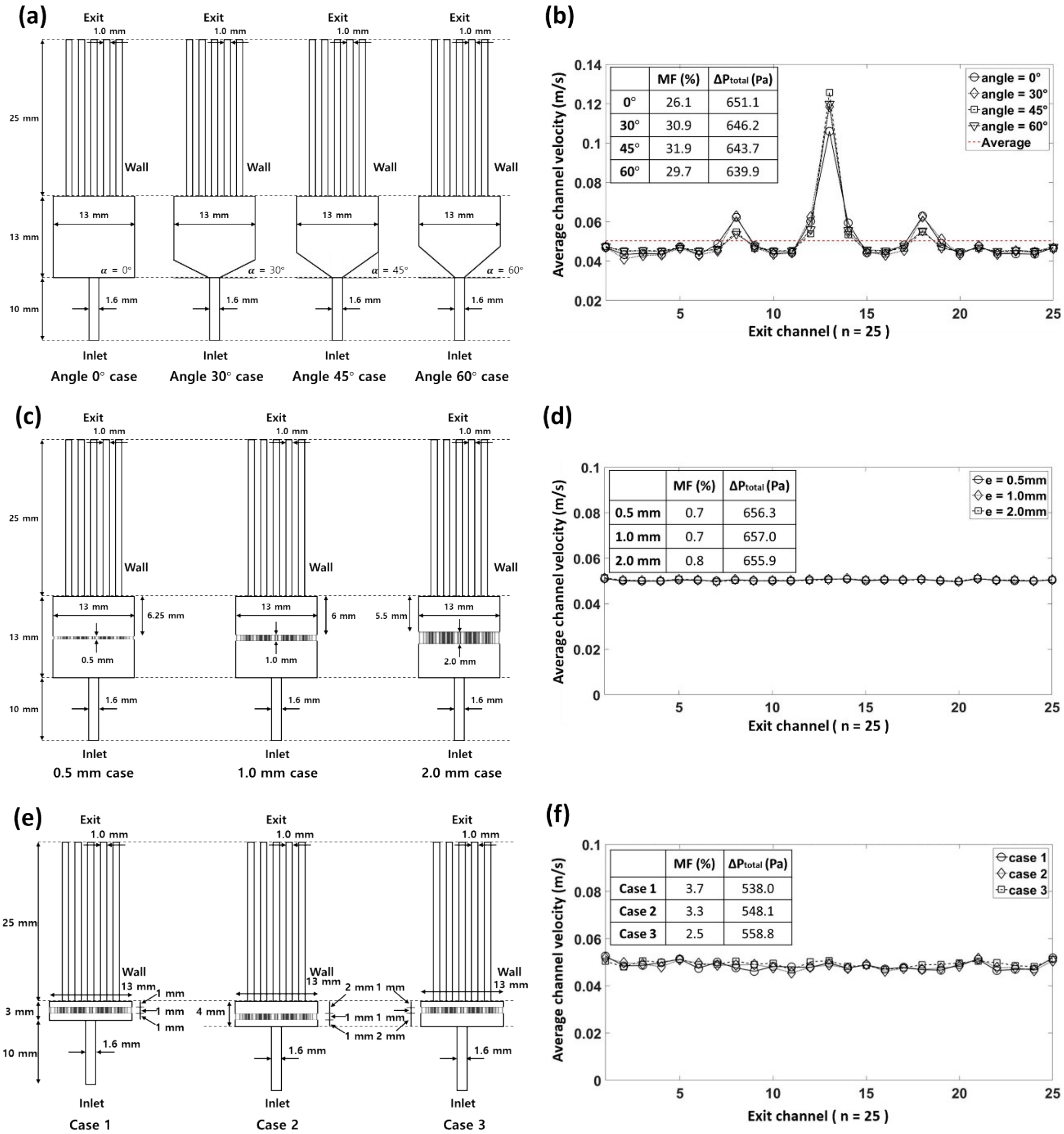

Fig. S2 Numerical simulation of flow distribution at 25 exit channels as a function of various parameters. (a, b) Entrance angle: ○ 0°; ◇ 30°; □ 45°; and ▽ 60°, (c, d) baffle thickness: ○ 0.5 mm; ◇ 1.0 mm; and □ 2.0 mm, and (e, f) different configurations of fluidic damper by positioning baffle structure at spatial ratio of the upper : baffle thickness : the bottom; ○ 1:1:1 mm (case 1) in 3 mm fluidic damper; ◇ 2:1:1 mm (case 2); and □ 1:1:2 mm (case 3) in 4 mm fluidic damper.

Table S1 Maldistribution factors (MF) and pressure drops as a function of various parameters, (a) entrance angle, (b) baffle thickness, and (c) different configurations of the fluidic damper

		MF (%)	ΔP_{in} (Pa)	ΔP_{damper} (Pa)	ΔP_{exit} (Pa)	ΔP_{total} (Pa)
(a)	Angle 0°	26.1	234.3	139.1	329.7	651.1
	Angle 30°	30.9	238.5	130.9	395.9	646.2
	Angle 45°	31.9	240.0	128.6	341.6	643.7
	Angle 60°	29.7	238.8	121.6	338.4	639.9
(b)	0.5 mm	0.7	235.7	217.9	286.2	656.3
	1.0 mm	0.7	236.1	224.6	285.7	657.0
	2.0 mm	0.8	235.7	250.1	285.7	655.9
(c)	Case 1	3.7	203.0	261.5	287.1	538.0
	Case 2	3.3	203.7	272.7	287.2	548.1
	Case 3	2.5	227.8	271.9	286.5	558.8

Table S2 Maldistribution factors (MF) and pressure drops as a function of baffle designs

	MF (%)	ΔP_{in} (Pa)	ΔP_{damper} (Pa)	ΔP_{exit} (Pa)	ΔP_{total} (Pa)
Design 1	2.5	227.8	271.9	286.5	558.8
Design 2	87.8	229.0	189.5	460.6	549.5
Design 3	13.9	228.7	260.2	329.6	557.9
Design 4	5.7	227.9	263.2	298.7	557.7
Design 5	3.3	227.9	265.8	287.1	560.0
Design 6	25.4	228.9	109.8	319.0	555.4
Design 7	87.4	228.9	168.7	447.0	548.8

4. Flow phenomenon depends on the position of the baffle

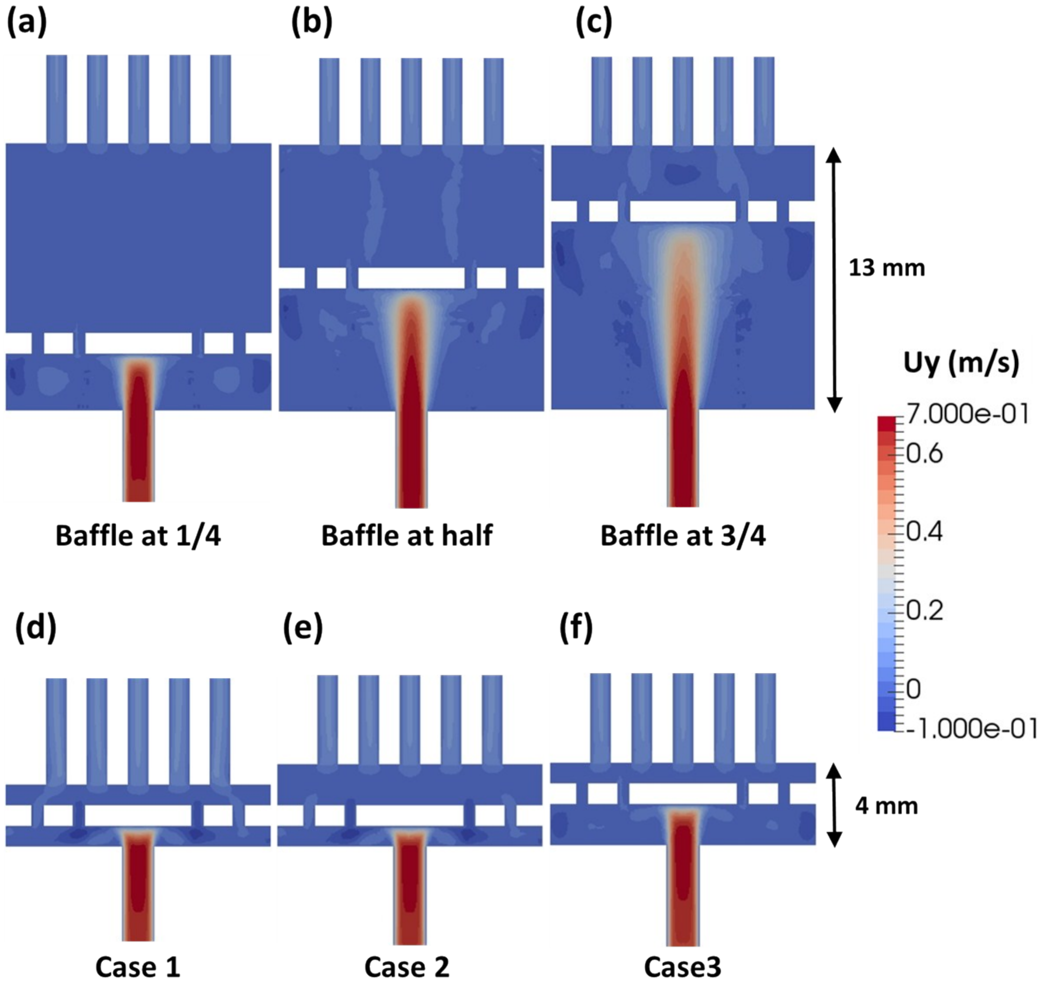

Fig. S3 Magnified cross-sectional contours of a y-directional velocity field: (a) The flow distributor equipped with a baffle located at 1/4 point of the fluidic damper; (b) the flow distributor equipped with a baffle located at the half of the fluidic damper; (c) the flow distributor equipped with a baffle located at 3/4 point of the fluidic damper; (d) the flow distributor of case 1; (e) the flow distributor of case 2; and (f) the flow distributor of case 3.

5. Detailed specification of flow distributors

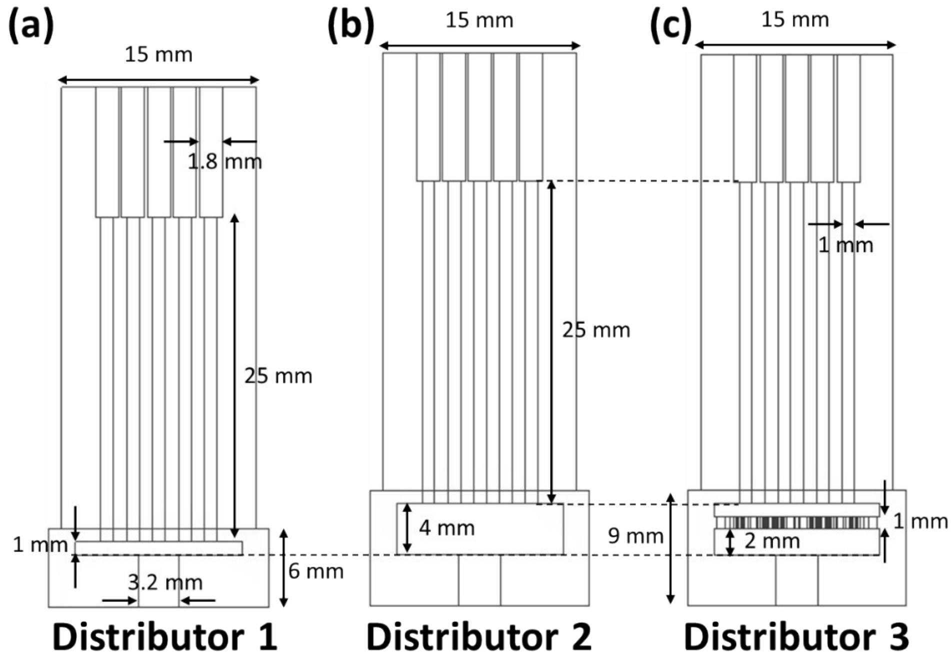

Fig. S4 CAD drawings with specific dimensions of different flow distributors: (a) distributor 1 has no fluidic damper, (b) distributor 2 has no baffle in the fluidic damper, and (c) distributor 3 is the optimized flow distributor.

6. Flow equalization effect by the baffle

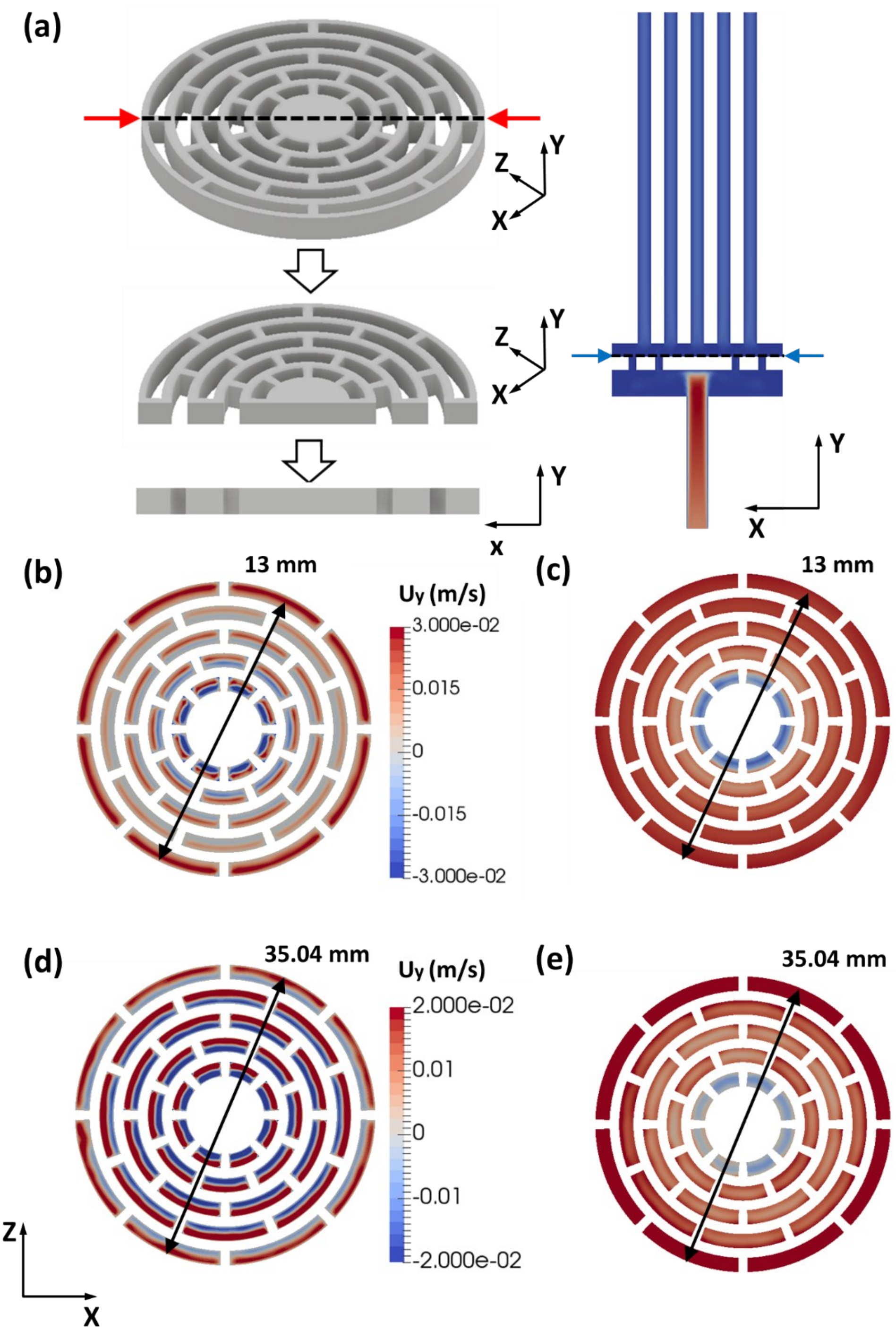

Fig. S5 (a) Full image and half-cut cross-sectional images of CAD design of the optimized baffle and the cross-sectional view of the flow distributor (red arrow: cutting line showing the position of the baffle seen in the cross-section of the flow distributor, blue arrow: cutting line showing the position of each cross-sectional view from (b) to (e)). (b) Contours of a y-directional velocity field and (c) pressure field of the optimized fluidic damper with 25 exit channels at the end of the baffle; and (d) contours of a y-directional velocity field and (e) pressure field of the fluidic damper with 625 exit channels at the end of the baffle.

7. Simulated performance of the optimized flow distributor at reduced flow rates

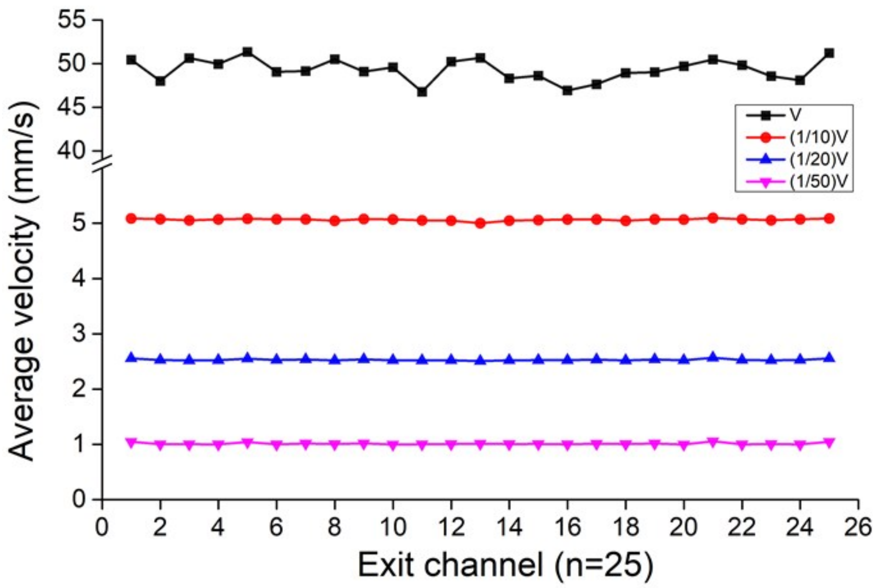

Fig. S6 Average velocity distribution of 25 exit channels under different flow rates: ■, original 60 mL/min; ●, 6 mL/min as 1/10 of 60 mL/min; ▲, 3 mL/min as 1/20 of 60 mL/min; and ▼, 1.2 mL/min as 1/50 of 60 mL/min.

8. The effect of the length of exit channels

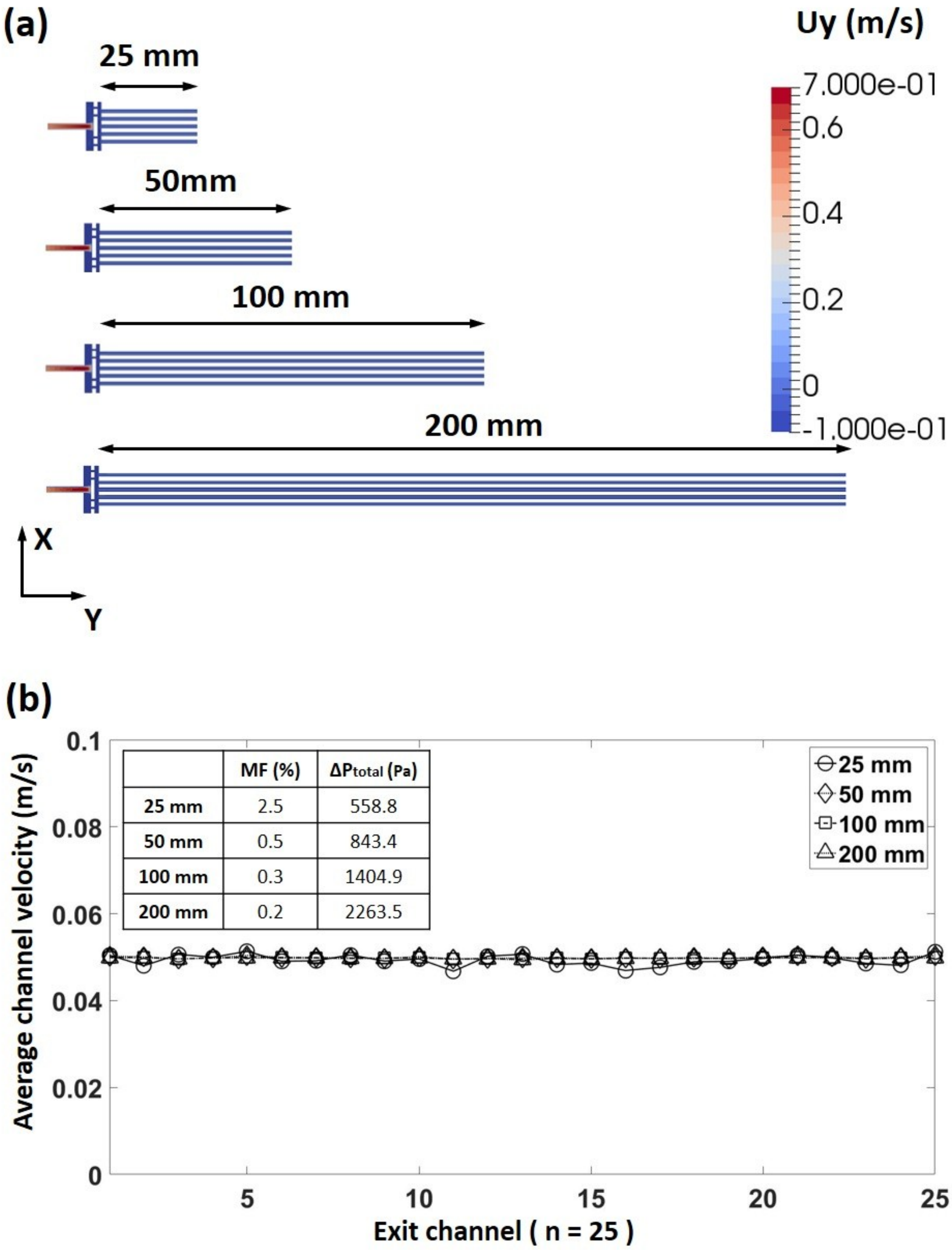

Fig. S7 (a) Contours of a y-directional velocity field of the optimized flow distributor according to the length of exit channels. (b) Average velocity distribution of 25 exit channels under different exit channel lengths: ○ the optimized flow distributor with exit channels of 25 mm; ◇ the optimized flow distributor with exit channels of 50 mm; □ the optimized flow distributor with exit channels of 100 mm, and △ the optimized flow distributor with exit channels of 200 mm.

Table S3 Maldistribution factors (MF) and pressure drops according to the length of exit channels

	MF (%)	ΔP_{in} (Pa)	ΔP_{damper} (Pa)	ΔP_{exit} (Pa)	ΔP_{total} (Pa)
25 mm	2.5	227.8	271.9	286.5	558.8
50 mm	0.5	226.4	267.8	571.4	843.4
100 mm	0.3	228.3	269.8	1132.6	1404.9
200 mm	0.2	227.8	269.8	2263.5	2534.6

9. Detailed information of 3D-printed flow distributors

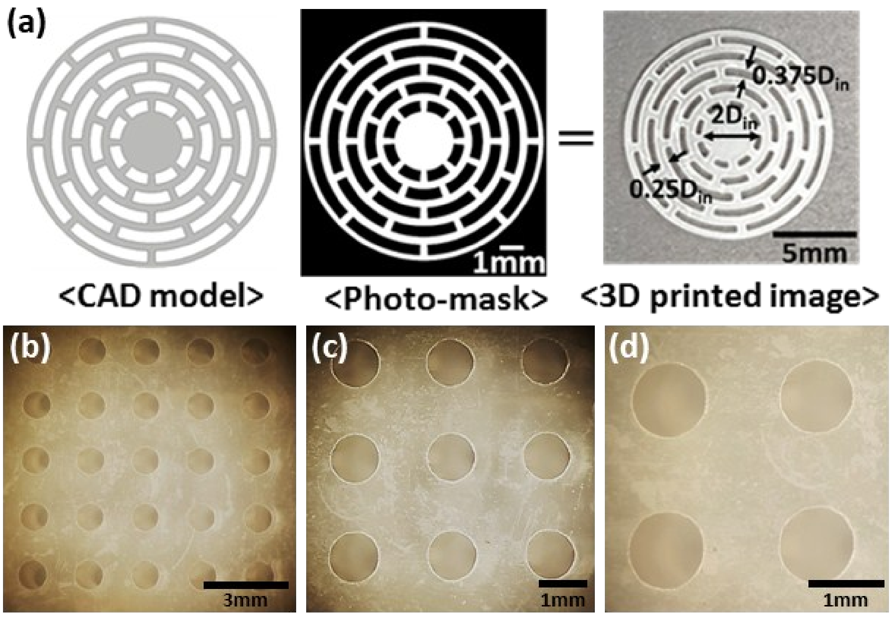

Fig. S8 (a) Baffles in CAD model, photo-mask, and 3D-printed image. Optical microscopic images from the cross-section of (b) 25 exit channels part, and (c) detailed 9 exit channels and (d) 4 exit channels.

Table S4 Uniformity of 3D printed 25 exit channels with 1 mm diameter, measured by 3D confocal scanning microscopy and the images (arrow: length of radius)

No.	Section	2D distance
1	3-point circle	496.297 um
2	3-point circle	505.694 um
3	3-point circle	508.093 um
4	3-point circle	495.157 um
5	3-point circle	497.306 um
6	3-point circle	494.063 um
7	3-point circle	493.063 um
8	3-point circle	493.009 um
9	3-point circle	491.524 um
10	3-point circle	490.594 um
11	3-point circle	498.273 um
12	3-point circle	505.087 um
13	3-point circle	505.117 um
14	3-point circle	507.634 um
15	3-point circle	506.551 um
16	3-point circle	508.684 um
17	3-point circle	505.119 um
18	3-point circle	501.452 um
19	3-point circle	498.853 um
20	3-point circle	493.318 um
21	3-point circle	494.764 um
22	3-point circle	495.366 um
23	3-point circle	502.264 um
24	3-point circle	501.834 um
25	3-point circle	508.659 um
Max.	-	508.684 um
Min.	-	490.594 um
Sum	-	12497.775 um
Average	-	499.911 um
Sigma	-	6.031 um
Count	0	-

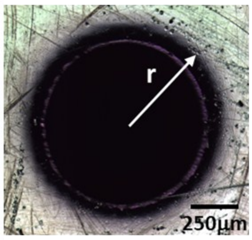

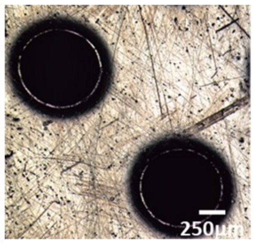

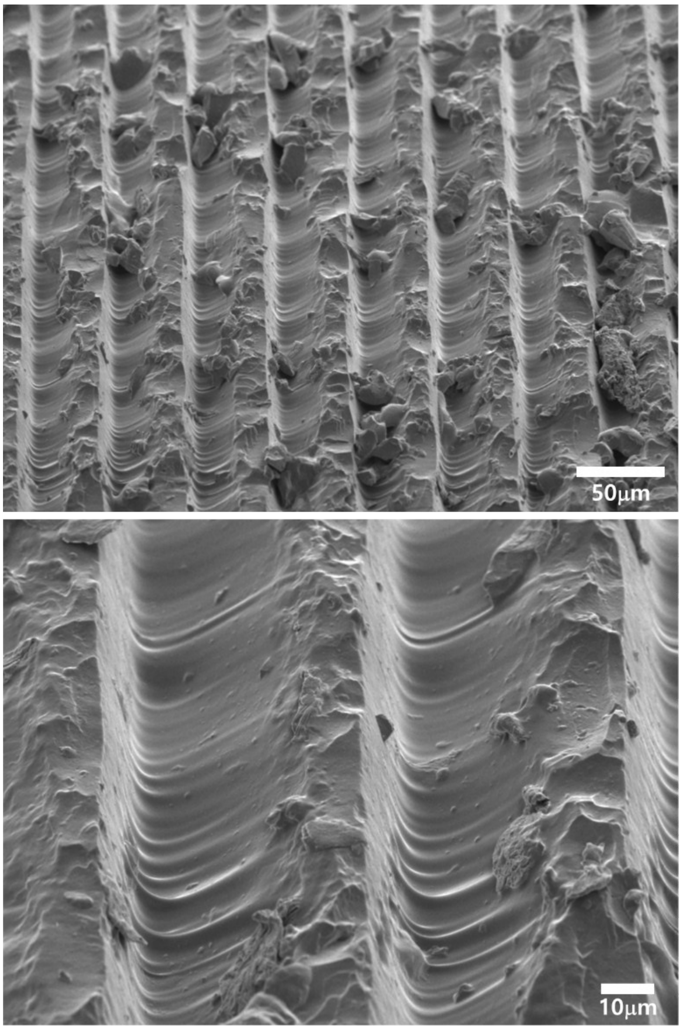

Fig. S9 Field emission scanning electron microscope (FE-SEM) images of the inner surface in the 3D-printed flow distributor.

10. Comparison between the experimental and the numerical results.

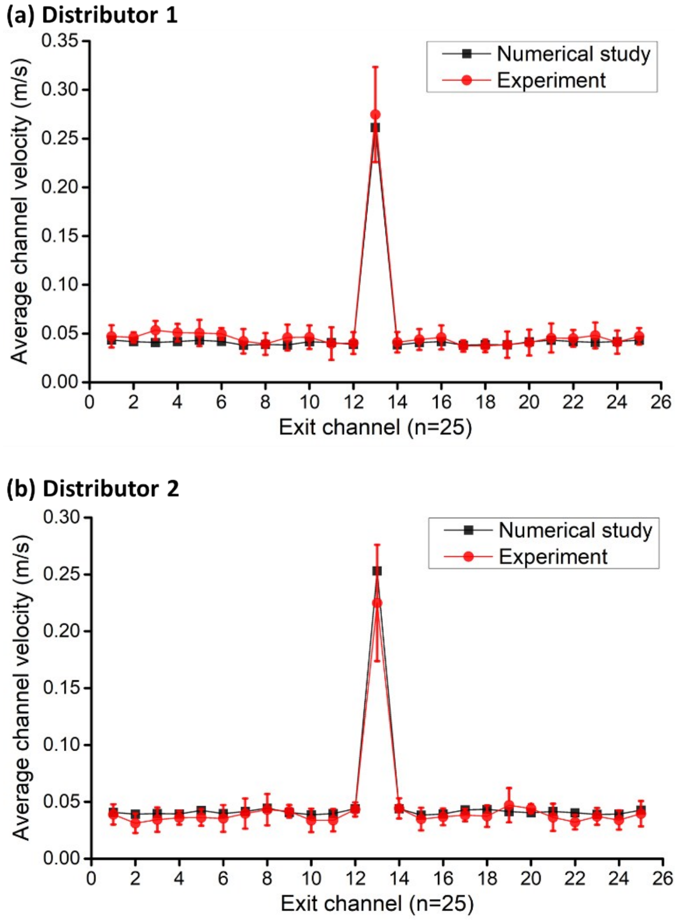

Fig. S10 Average velocity distribution of 25 exit channels in the case of (a) distributor 1 and (b) distributor 2: ●, Experiment and ■, numerical study.

Table S5 Summary of simulated MFs and pressure drops for three types of distributors and their experimental results.

	MF (%)		ΔP_{in} (Pa)	$\Delta P_{spacing}$ (Pa)	ΔP_{damper} (Pa)	ΔP_{exit} (Pa)	ΔP_{total} (Pa)
	Exp.	Num.	Numerical	Numerical	Numerical	Numerical	Numerical
Distributor 1	86.4	89.0	222.5	172.8	N/A	479.0	528.6
Distributor 2	82.8	85.8	229.5	N/A	180.0	453.0	549.3
Distributor 3	2.2	2.5	227.8	N/A	271.9	286.5	558.8

11. Performance evaluation of the optimized flow distributor.

Table S6 Comparative efficiency of the fabricated flow distributor with the reported works.

Ref.	Study type	Number of channels	Application	Flow distribution uniformity
Present work	N, E	25, 625	Stacked microreactor	MF: (N) 2.5 %, (E) 2.2 % in 25 exit channels at inlet velocity = 0.497 m/s, Re = 891 (N) 1.2 % in 625 exit channels at inlet velocity = 0.332 m/s, Re = 1,485
1	N	10	Parallel microchannels	MF: (a) 23.3 % (b) 24.3 % at inlet velocity = 0.125 m/s, Re = 125 (c) 38.7 % (d) 39.5 % at inlet velocity = 1.25 m/s, Re = 1,250
2	N, E	90	Parallel mini-channels	MF: (a) 13.8 % at Re = 100 (b) 17.2 % at Re = 1,000
3	N	225	Parallel stacked microreactor	MF: (a) 2.6 %, (b) 2.8 %, (c) 3.5 %, (d) 7.2 %, (e) 10.9 %, (f) 18.4 %, (g) 27.5 %, (h) 42.7 % and so on at inlet velocity = 0.127 m/s
4	N, E	21	Heat exchanger	MF: (a) N = 112.4 %, E = 121.0 % (b) N = 37.1 %, E = 30.7 % (c) N = 12.6 %, E = 20.9 % at Re = 60,000

N: numerical study; E: experimental study; MF: maldistribution factor defined in Eq. (2); Re: Reynolds number

References

1 C. Pistoresi, Y. Fan and L. Luo, *Chem. Eng. Process. Process Intensif.*, 2015, **95**, 63-71.

2 M. Saber, J. Commenge and L. Falk, *Chem. Eng. Sci.*, 2010, **65**, 372-379.

3 C. Pistoresi, Y. Fan, J. Aubril and L. Luo, *Chem. Eng. Process. Process Intensif.*, 2018, **123**, 67-81.

4 J. Wen, Y. Li, A. Zhou and K. Zhang, *Int. J. Heat Mass Transf.*, 2006, **49**, 1667-1678.

12. Flow distribution performance of a bifurcation flow distributor.

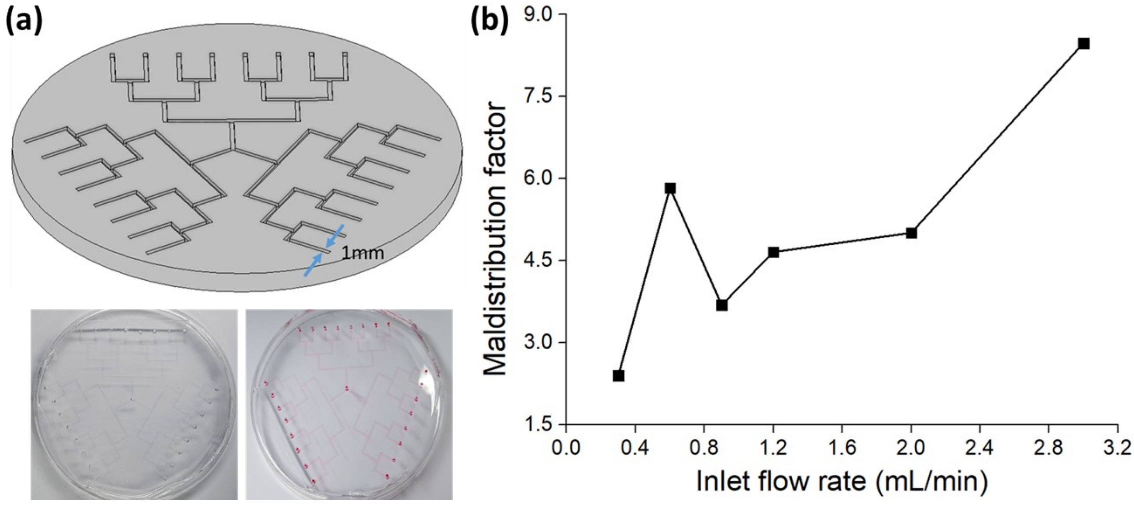

Fig. S11 Flow distribution performance of a 24 bifurcations flow distributor. (a) CAD design of the bifurcation flow distributor and the fabricated device. (b) Effect of the flow rate at 0.3, 0.6, 0.9, 1.2, 2 and 3 mL/min on the performance of the bifurcation flow distributor.